Materials Chemistry and Physics 167 (2015) 181–187

Contents lists available at ScienceDirect

Materials Chemistry and Physics

journal homepage: www.elsevier.com/locate/matchemphys

The role of amine derivatives in the formation of hierarchical Pt micro/nanostructures

M.D. Johan Ooi [a, *], A. Abdul Aziz [a, b]

[a] Nano – Optoelectronic Research and Technology (N.O.R) Laboratory, School of Physics, Universiti Sains Malaysia, 11800 Minden, Penang, Malaysia
[b] Nanobiotechnology Research and Innovation (NanoBRI), INFORMM, Universiti Sains Malaysia, 11800 Minden, Penang, Malaysia

HIGHLIGHTS

- Pt flower-like structure was produced using amino alcohol via solvothermal method.
- Pt assisted DEA exhibit higher reducing rate compared to MEA.
- The synthesis times play a critical role in the development of Pt structures.
- Pt produced in the 5th hour (DEA) exhibit slow current decayed at longer times.
- Pt particles formed in the 7th hour (MEA) exhibit excellent catalytic activity and stability.

ARTICLE INFO

Article history:
Received 16 April 2015
Received in revised form
27 September 2015
Accepted 13 October 2015
Available online 23 October 2015

Keywords:
Metals
Chemical synthesis
Crystallography
Electrochemical properties

ABSTRACT

We discussed the formation of platinum hierarchical micro/nanostructure by varying the synthesis time using two amine derivatives, e.g. Monoethanolamine (MEA) and Diethanolamine (DEA) as the reducing agent. This work shows that the amine derivatives play a crucial role in controlling the reducing rate as Pt synthesised with DEA exhibited the fastest growth process whilst the synthesis time influences the development of Pt anisotropic structures. With a shorter synthesis time of 5 h, both particles synthesised using MEA and DEA exhibit small flower-like structures, while a larger network of flower-like microstructure was established at 9 h. The optimum condition for Pt assisted MEA and DEA is 7th hour for MEA and 5th hour for DEA. The particles produced using DEA during the 5th hour of synthesis time had a large electrochemical surface area (5.90 $cm^{-2}g^{-1}$), high catalytic activity and greater tolerance against CO adsorption. For particles synthesised with MEA, at the 7th hour, the reaction produces bigger flower-like particles comprised of collective triangular petals having 4.88 $cm^{-2}g^{-1}$ electrochemical surface areas and exhibit greater stability at a longer period.

1. Introduction

Platinum (Pt) is a precious transition metal with great electrical conductivity, catalytic property, is resistant to corrosion and physically stable at high temperature. Therefore, it was widely applied in industrial and environmental applications such as biosensor [1], alloying agent in some metal products (e.g. medical instruments, electrical contacts and thermocouple), as a catalyst in fuel cell industries [2], and reducing pollutant emission from automobiles. However, its limited resource makes Pt very expensive. Therefore, the major challenges are to increase its catalytic activity and reduce Pt consumption. One approach to solve these problems is by synthesising specific micro/nanostructures as the shape and size known to exhibit a remarkable influence on its properties [3].

Pt hierarchical micro/nanostructures became a subject of interest over the last few years. Its complex geometry offers advantages of high surface area, synergistic interaction between adsorbed molecules and excellent electro-catalytic performances. Among the various hierarchical structures produced are hollow nanostructures [4], nanowires [5,6], nanostars [7], Y junction nanostructures [8] and nanoflowers [9]. Nonetheless, producing these geometrical shapes remains a challenge because of their high surface energy that tends to preserve its shape at the lowest surface

* Corresponding author.
E-mail addresses: mdjo13_phy062@student.usm.my (M.D. Johan Ooi), lan@usm.my (A. Abdul Aziz).

http://dx.doi.org/10.1016/j.matchemphys.2015.10.028
0254-0584/

energy. Several techniques were developed to produce these hierarchical structures and chemical routes are the most preferable technique due to easy handling, high yield, economical, and allow for controlling variations of experimental parameters. Among the recognised parameters varied in most experiments are the temperatures, the nature of surfactants, precursor's concentration, type of solvents and reducing agent.

Recently, amino based surfactant was extensively investigated for its dual properties as surfactants and as a reducing agent. For instance, Huang et al. [10] synthesised octapod polyhedral nanoparticles using methylamine to reduce $PtCl_6^{2-}$ to Pt^0. Its derivative, which is amino alcohol, has a similar function. However, limited studies were made to date. Concerning shape transformation, the effect of synthesis time on the growth of Pt nano/microstructures can be an important experimental condition that needs to be examined. Knowledge on the growth development is critical in order to understand the mechanism of the formation of a hierarchical structure and to further improve synthesis protocol. More importantly, there is no study regarding the use of amino alcohol, especially monoethanolamine (MEA) and diethanolamine (DEA) as reducing agents were reported, in particular in regards towards preparation of Pt hierarchical nano/microstructures. We believe that MEA and DEA may have a strong influence on the synthesis time in producing Pt nano/microstructures that is better or equivalent to the one produced by other methods/reducing agents. Therefore, we put an initiative to study the effect of MEA and DEA in the synthesis with emphasis on the variation of synthesis time as well as discussing its relationship particularly on structural, morphological and catalytic properties of Pt.

2. Experimental procedure

Hexachloroplatinic acid (H_2PtCl_6, 8 wt% in aqueous solution), polyvinylpyrrolidone, (Molecular weight 40 000), Platinum black and Nafion® 5 wt% were bought from Sigma Aldrich. N, N Dimethylformamide (DMF) from Merck and both monoethanolamine (MEA) and diethanolamine (DEA) from R&M Chemicals. All of the chemicals were used as received without further purification.

The experimental procedure of this work is motivated by the growth process proposed by Huang et al. [10] with some modification made by replacing methylamine solution with monoethanolamine (MEA). MEA and DEA are the preferred chemicals because they exhibit similar functions, but are less hazardous compared to methylamine. In a typical synthesis, 0.50 ml H_2PtCl_6 was added into 10 ml DMF, followed by 0.17 ml MEA (2.8 mmol) and 0.2 g PVP under vigorous mixing to produce a homogeneous yellow solution. Next, the solution was transferred to Teflon-lined stainless steel autoclave reactors and heated from room temperature to 160 °C for 5,7 and 9 h. Next, the solution was precipitated with acetone and separated via centrifugation. The product was collected by discarding the yellowish supernatant and washed three times by precipitation/dissolution with acetone/ethanol solvents to remove any by-product. The product was redispersed in ethanol for characterisation. Finally, these protocols were repeated by replacing MEA with DEA for comparison.

The morphologies of the synthesised Pt particles were analysed using a field emission scanning electron microscope (NOVA Nanosem 45) with an acceleration voltage of 5 kV. The structural properties were characterised using X-ray diffractometer (Bruker D8 Advance Diffractometer) operating at a wavelength of 1.54056 Å by CuKα radiation. The Fourier transform IR (FT- IR) spectroscopy were characterised using FT-IR ATR Perkin Elmer. The electrochemical characterisation was performed using eDAQ (ER466) integrated potentiostat utilising a conventional three electrode system with glassy carbon serves as the working electrode, Pt rod as counter electrode and saturated calomel electrode (SCE) as the reference electrode.

The working electrode was prepared by transferring 5 μL of the colloidal Pt on the glassy carbon electrode (Ø = 3.0 mm), which was polished earlier with γ-Al_2O_3 (0.3 μm and 0.05 μm) and dried with N_2 flow prior to use. Nafion® (0.05 wt%, 3 μL) solution was then pipetted onto the Pt film and dried overnight in an ambient environment before performing the electrochemical measurements. The hydrogen adsorption/desorption analysis was studied using cyclic voltammetry in 0.5 M H_2SO_4 at −0.25 V and 1.3 V. The electrooxidation of formic acid (HCOOH) was examined for 20 cycles in 0.5 M H_2SO_4 + 0.25 M HCOOH at −0.25 V and 1.2 V. Both measurements used a potential sweep rate of 50 mV/s. The chronoamperometry measurement was made at 0.67 V (versus SCE) in 0.5 M H_2SO_4 + 0.25 M HCOOH in 1000 s.

3. Results and discussion

Fig. 1 represents the FE-SEM micrographs of the synthesised Pt particles at a different reaction time. At the 5th hour of synthesis time, small particles with spiky features were observed for Pt prepared with both MEA and DEA. Highly close-packed particles were produced on particles synthesised with DEA, whilst a less-packed particle was produced on MEA. At the 7th hour, both samples prepared by MEA and DEA developed a combination of flower-like particles along with coalescence of the particle. As the synthesis time approached the 9th hour, the flower-like structures of both samples were grown into a large flower network.

The reaction mechanism can be proposed as below:

Monoethanolamine

$$PtCl_6^{2-} + NH_2CH_2CH_2OH \rightarrow PtCl_4^{2-} + NH_2CH_2CHO + 2H^+ + 2Cl^- \quad (1)$$

$$PtCl_4^{2-} + NH_2CH_2CH_2OH \rightarrow Pt^0 + NH_2CH_2CHO + 2H^+ + 4Cl^- \quad (2)$$

Diethanolamine

$$PtCl_6^{2-} + NH(CH_2CH_2OH)_2 \rightarrow PtCl_4^{2-} + NH(CH_2CHO)_2 + 4H^+ + 2Cl^- \quad (3)$$

$$PtCl_4^{2-} + NH(CH_2CH_2OH)_2 \rightarrow Pt^0 + NH(CH_2CHO)_2 + 4H^+ + 4Cl^- \quad (4)$$

First, the reaction commences with a reduction of Pt (IV) to Pt (II) via hydrogen from the alcohol group of MEA and DEA. Next, the Pt (II) was subsequently reduced to Pt (0) from the nascent releases of Hydrogen (H) and the remaining amino alcohol. Both of them are amino derivative, (therefore, a weak reducing agent); thereby, only capable of producing a slow reduction rate and slow nucleation process. However, the reaction with DEA releases 4 mol of hydrogen atoms, which is two times the amount of hydrogen released by MEA. Therefore, a reaction with DEA likely increases the reducing rate of Pt, thereby speeding up the nucleation and growth process. These possibly explain highly close-packed distribution of particles and rapid formation of flower-like structure on samples synthesised with DEA. Next, the formation mechanism proceeds with autocatalytic growth to form nuclei that further collide with Pt ions, atoms or cluster to form a stable seed. In principle, the face centred cubic Pt structures possess surface energies in a sequence of $\gamma_{\{111\}} < \gamma_{\{100\}} < \gamma_{\{110\}}$. Therefore, the seed has a tendency to form a

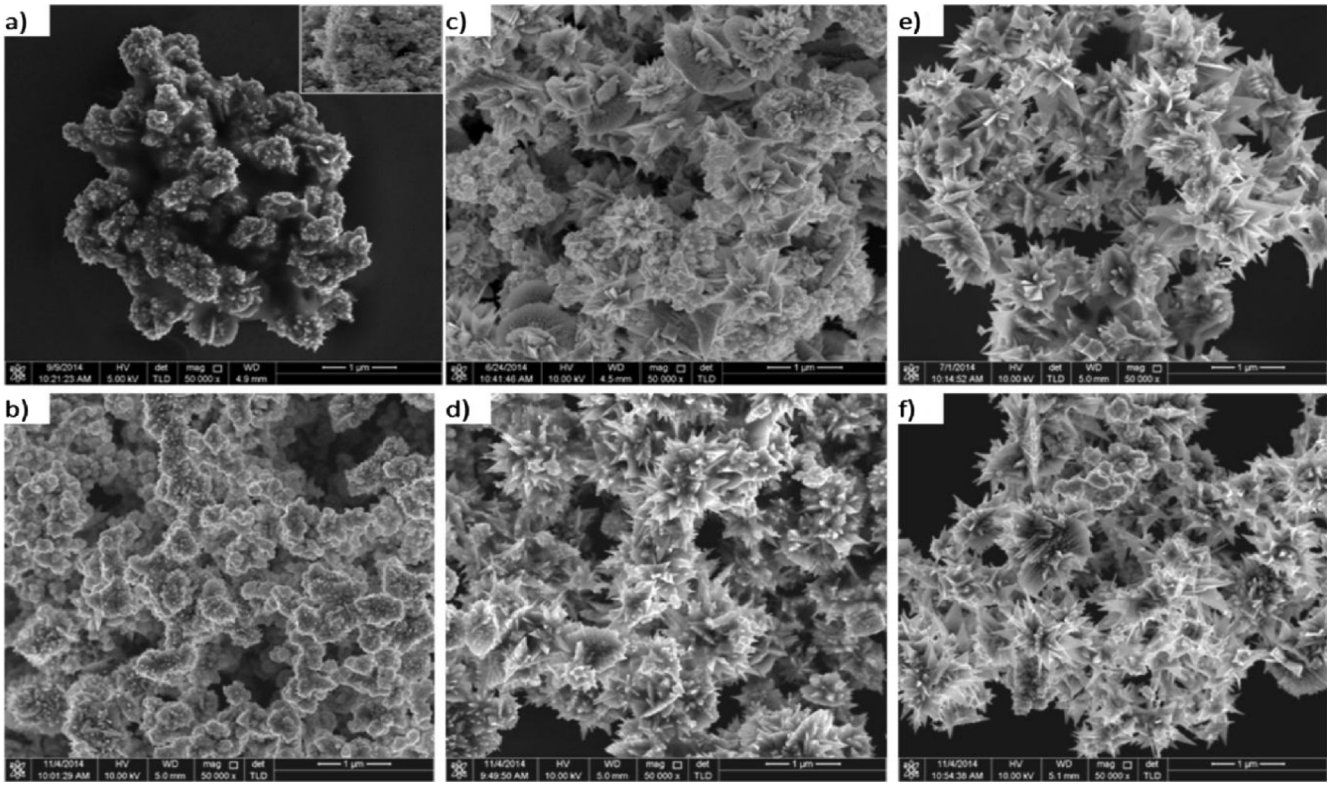

Fig. 1. FE-SEM images of the synthesised Pt hierarchical micro/nanostructures at 5, 7 and 9 h respectively a–c) MEA and d–f) DEA. Inset Fig. 1a) is the image of the commercial Pt black.

particle surface enclosed by a mix of {111} and {100} facets to minimise its total surface energy [11]. Because the reduction rate is slow and obeys the lowest energy principle, the anisotropic growth along the closed packed <111> direction is more favoured and produces various spiky structures. The shorter duration synthesis at the 5th hour likely induced a high concentration of metal salts, which produce instability in the overall particle surface charge. Therefore, leading to particles' agglomeration [12] as observed in Fig. 1a and 1d.

When the growth time reaches the 7th hour, the high supersaturation state further develops the spike structure into a triangular petal and produce flower-like pattern. The large distribution of flower-like morphology is clearly observed in the sample synthesised with DEA. This therefore supports the idea that DEA increases the reducing rate, produced more seeds and accelerates the formation of flower-like particles. In contrast, Pt synthesised with MEA developed less flower-like structures, which suggested that the nucleation rates of MEA are slower than DEA. For MEA, fully grown flower-like structures are only attained after the 9th hour of reaction. This duration is the time period needed to achieve a metastable state for crystals to grow without the interruption of nucleation. In contrast, Pt synthesised with DEA experiences a fast nucleation and crystals growth. Therefore, the longer duration time induced the flower to grow bigger. This formation, possibly driven by dissolution of smaller crystals that incorporate into surface of larger particle [13].

The X-ray diffraction pattern of the amine assisted growth Pt particles at respective time is presented in Fig. 2. Based on JCPDS data card 00-001-1194, all of the samples represent face centred cubic structures. No other peak of impurities detected implies that the synthesised Pt is a pure polycrystalline crystal. The broaden hump displayed at $2\Theta = 24^{\circ}$corresponds to the glass slide used as the substrates.

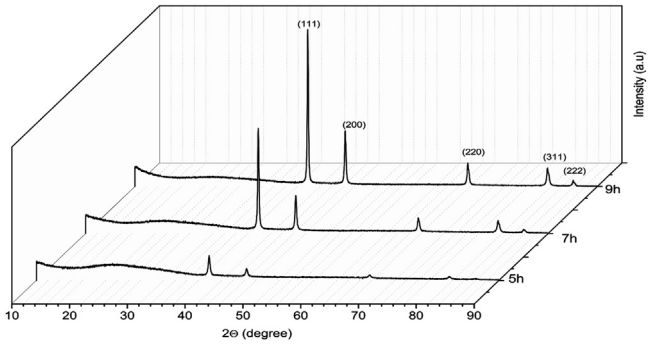

Fig. 2. X-ray diffraction of the Pt particles synthesised with MEA and DEA at various synthesis hour.

The X-ray diffraction pattern for Pt synthesised with MEA and DEA are identical related to synthesis hour. It can be seen that the XRD peaks show a significant increase in intensities in longer hours, suggesting a high concentration of Pt atoms residing on the plane. The narrow width and sharp reflection peaks at the 7th and 9th hour, which indicate improvement of crystallinity for Pt synthesised with MEA and DEA. At the 5th hour, the low diffraction peaks imply a low degree of atomic concentration. Taking the strongest line which is the (111) reflection peak, the average crystallite size for the 5th hour is approximately 26 nm, the 7th hour is ~34 nm and the 9th hour is about 36 nm (calculated by Debye-Scherrer formula [14]). The increment of crystallites' size shows that the growth of crystallite size is time dependent. As the synthesis time is extended, the probability of atoms adhering into the surface of the crystal by gradient diffusion is higher, driven by the differences between their concentration in the bulk suspension and

near crystal surface. Therefore, resulting in an increase in particle size [15].

FTIR characterisation is employed to identify the organic chemical compound remains on the particles and suggest a possible interaction of the species involved.

The FTIR spectra of the synthesised Pt particles compared to its pure chemical are shown in Fig. 3. Both of the synthesised samples assisted MEA and DEA show a similar IR profile with their pure chemical. Both of the synthesised Pt exhibits a broad peak at 3322 cm^{-1} (DEA) and 3330 cm^{-1} (MEA) corresponds to a hydroxyl group (O–H) of hydrocarbon solvent in which the Pt was dispersed. The absorption bands at 2973 cm^{-1} (DEA), 2978 cm^{-1} (MEA), and 1381 cm^{-1} correspond to the stretching vibration modes and C–H bend of the methylene groups ($-CH_2-$) respectively [16]. Peaks at 1646 cm^{-1} (MEA), 1665 cm^{-1} (DEA), 1066 cm^{-1} (DEA) and 1089 cm^{-1} (MEA) are due to the N–H bend absorption and C–N bend of the amine group respectively. The existence of these peaks indicates that the amine was indeed attached to Pt surface. However, there are no significant peaks corresponding to N–H stretch (~3310–2990 cm^{-1}) [15] suggesting that the hydrophilic head ($N-H_2$) was not fully binding to the Pt particles. The strong and intense peak at 1043 cm^{-1} is assigned to the stretching vibration of C–O whilst the peak at 880 cm^{-1} (DEA) and 884 cm^{-1} (MEA) are attributed to O–H bend vibration modes of the alcohol group. There are no absorption peaks of (C=O) of N-vinylpyrrolidone suggesting that PVP is not attached to Pt facets and was removed in the washing process.

It is known that the geometrical shape exerts a strong influence on the catalytic activity of Pt. In particular, the electrochemical surface area (ECSA) represents the intrinsic catalytic activity of the catalyst, which can be estimated based on the following formula [17]:

$$ECSA = \left(\frac{Q_H}{0.21L}\right) \quad (5)$$

Where Q_H is the average of the integrated charge from the voltammogram of the adsorbed/desorption hydrogen on the CV curve (mC). 0.21 mC/cm^2 is the charge needed to reduce a monolayer of hydrogen adsorption and L (g/cm^2) is the Pt loading on the electrode. From the experiment, the measured ECSA are listed in Table 1.

The increment of ECSA value for a sample produced at a longer synthesis hour suggests that size and shape have a strong influence on the catalytic activity of the Pt. The sample that was prepared for 5 h exhibited the smallest ECSA value, probably due to an effect of low active area deriving from the agglomeration of particles. Whereas the increment of ECSA value for Pt prepared for the 7th and 9th hour was probably instigated by their multidimensional structure that were comprised of rich {111}, {100} and {110} specific facets or plane. In contrast to MEA, Pt synthesised with DEA exhibiting a decreasing value of ECSA at a longer duration hour indicative that an excess and large flower network induces hindrance by suppressing the surface area and its active site. It is interest to see that Pt prepared with DEA for the 5th hour had the highest ECSA value suggesting that the combination of closely packed and spiky structure produced large surface active sites. However, the ECSA value of the as-prepared Pt particles is much lower compared to Pt black (32.22×10^{-2} m^2/g, calculated by a similar method) is possibly due to the presence of the adsorbed organic amine species which hinder its active site. The catalytic properties of the synthesised particles associated with their geometry can be further confirmed by cyclic voltammetry measurements.

The electrochemical response of the synthesised Pt particles was compared to commercial Pt black using acidic media 0.5 M H_2SO_4. The characteristic of the CV curve from all samples is almost identical to the peak shape of Pt black, an indication of a

Table 1
Calculated ECSA of the synthesised Pt particles.

Synthesis time	ECSA MEA ($(\times 10^{-2})$ m^2/g)	ECSA DEA ($(\times 10^{-2})$ m^2/g)
5H	0.54	5.90
7H	4.88	0.55
9H	4.43	0.79

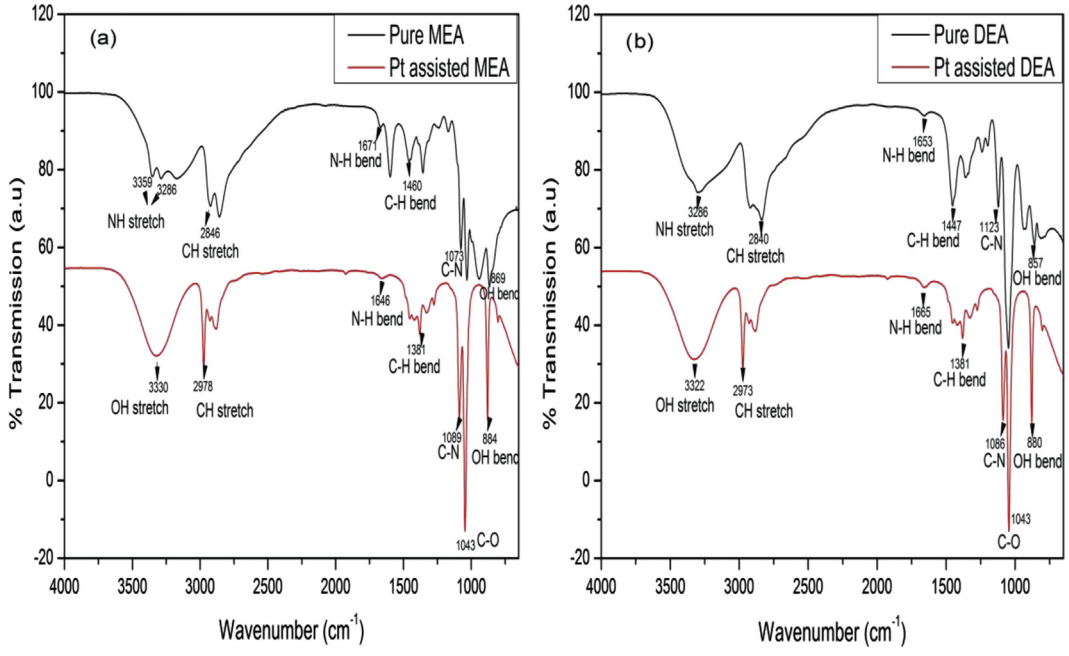

Fig. 3. FTIR spectra of the synthesised Pt particles a) assisted MEA and pure MEA; b) assisted DEA and pure DEA.

polycrystalline surface nature [18]. The charges associated with hydrogen adsorption/desorption (−0.25 − 0.1 V) [19] and the oxidation/reduction of the Pt (0.1–1.25 V) were observed in all the samples. In detail, the peak between 0.1 V and 0.8 V corresponds to the double layer charge of the oxygenated species on the surface of carbon electrode [20].

At potentials greater than 0.8 V, the CV curve profile represents the process of Pt (II) oxides formation. In the backward potential scan, Pt was reduced from Pt (II) oxides to Pt (0). The corresponding oxygen reduction peaks for PtO were observed at 0.5 V.

The multiple peak observed in hydrogen adsorption/desorption region shows that there are multiple exposed crystallographic planes, while, the slightly shifted peak position with respect to Pt black was probably due to the surface effect of a different orientation [21]. The decreased peak intensities were directed from inhibition of some active site due to an existence of amine organic species, agglomeration of particles and dense collection of flowers. However, among the synthesised samples, Pt prepared with DEA at 5 h (Fig. 4b) exhibited a well-defined oxygen reduction peak which infers high reduction activity of the synthesised Pt.

Cyclic voltammogram of formic acid electrooxidation of the synthesised Pt are shown in Fig. 5. In the forward − going scan, two anodic peaks were observed for all of the samples. The first peak at ~0.3 V is associated with oxidation of HCOOH to CO_2,I_p^d (dehydrogenation pathway) and the second peak at ~ 0.7 V corresponds to oxidation of the CO to CO_2, (I_p^{ind}). The adsorbed CO was constituted from the non-faradaic dissociation of formic acid [22] and was considered a "poison" to Pt, because it inhibits the catalytic active sites and reduces the catalyst performance. In the reverse - going scan, one peak stretching from 0.5 V to 0.1 V is observed mainly associating with oxidation of formic acid on Pt surface free from oxygenated species (I_b). During this reverse sweep scan, most of the adsorbed CO were oxidised and removed from the Pt surface, which makes the oxidation of formic acid obeying direct dehydrogenation pathway.

The level of Pt surface poisoning by CO can be estimated using the I_p^d/I_p^{ind} ratio while the degree of tolerance against CO poisoning can be estimated using I_p^d/I_b [22] ratio which is summarised in Table 2. Based on Table 2, the I_p^d/I_p^{ind} ratio for both Pt synthesised with MEA and DEA decreased at longer synthesis hours indicating a poor catalytic activity toward formic acid oxidation. The ratio reduction is probably due to the large flower network that induces CO accumulation and promotes the Pt to catalyse via indirect oxidation pathway. In contrast, the small flower-like structures (5 h) presumably suppress CO adsorption, therefore producing excellent catalytic activity and promoting direct oxidation.

The ratio I_p^d/I_b of MEA samples are on a decreasing trend whereas DEA samples are increasing under a prolonged synthesis hour. The decreasing ratio of MEA at the longer hour suggests a low degree of tolerance against the poisoning CO adsorption and low efficiency in oxidizing formic acid to CO_2. It is worth to note that a I_p^d/I_b ratio equal to 1 depicts high catalytic activity for formic acid oxidation in the forward and backward potential scan which is an ideal characteristic for fuel cell fabrication [22]. However, $I_p^d/I_b\rangle 1$ is a sign of poor catalytic behaviour because only a partial reduction of Pt−O takes place [23], and may be due to a restriction of active sites to reduce Pt (II) oxide to Pt. Comparing to commercial catalyst (I_p^d/I_p^{ind}= 0.23 and I_p^d/I_b = 0.32), the catalytic activity of the synthesised Pt (MEA and DEA) at the 5th hour is higher than the commercial Pt, an indicative that the structures produced is more receptive towards formic acid electrooxidation and has greater tolerance against CO adsorption despite of having a low value of ECSA. The better catalytic activity of the present Pt is probably contributed by the recovered active sites of the adsorbate organic amine species, thus increase its electro-catalytic reaction.

The catalytic stability of the prepared Pt was analysed by chronoamperometry measurements in Fig. 6. As shown, the current density rapidly declined within the first few minutes, probably due to the formation of double layer capacitance and adsorption of CO on the Pt surface until it reaches equilibrium of surface coverage [20].

All of the samples exhibited a high initial current except for the sample prepared with DEA at the 7th hour and 9th hour, which supported the low efficiency in catalytic performance. The current

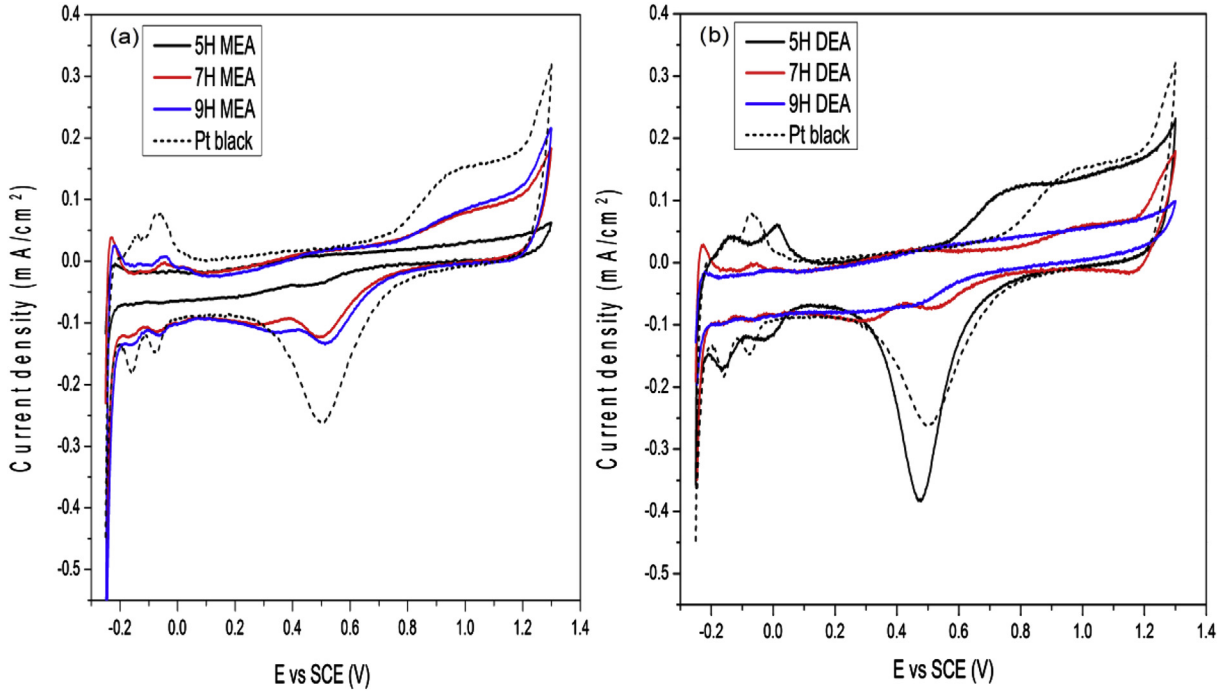

Fig. 4. Cyclic voltammogram curves of the synthesised Pt in 0.5 M H_2SO_4 solution a) MEA and b) DEA at different synthesis time.

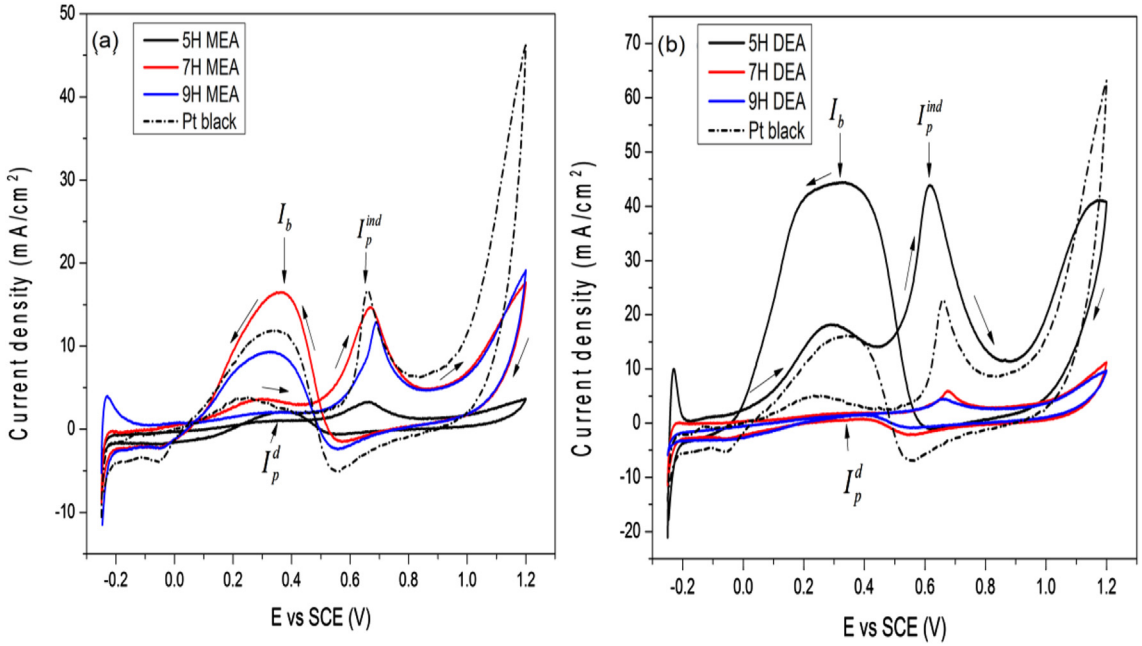

Fig. 5. Cyclic voltammogram of formic acid electrooxidation in 0.5 M H_2SO_4 solutions at potential scan rate of 50 mV/s. Pt synthesised assisted a) MEA and b) DEA at different synthesis time.

Table 2
Current density and ratio of the electrooxidation of formic acid of the synthesised Pt at variation hours (h).

MEA						DEA				
h	I_p^d (mA/cm^2)	I_p^{ind} (mA/cm^2)	I_b (mA/cm^2)	I_p^d/I_p^{ind}	I_p^d/I_b	I_p^d (mA/cm^2)	I_p^{ind} (mA/cm^2)	I_b (mA/cm^2)	I_p^d/I_p^{ind}	I_p^d/I_b
5	0.98	3.35	2.25	0.29	0.44	18.21	43.85	44.55	0.42	0.41
7	3.78	14.77	16.58	0.26	0.23	2.16	5.85	0.76	0.37	2.84
9	1.97	12.93	9.29	0.15	0.21	1.93	4.68	1.46	0.41	1.32

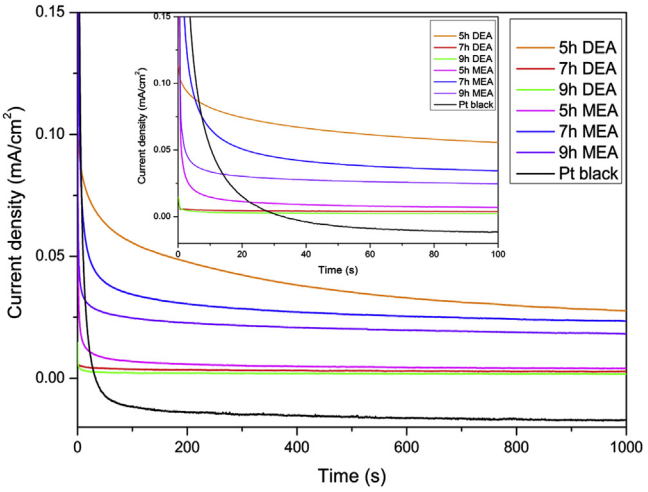

Fig. 6. Chronoamperometry diagrams of the synthesised Pt in 0.5 M H_2SO_4 containing 0.25 M HCOOH measured at 0.67 V in 1000 s. Inset figure shows a different time scale (0–100 s) to facilitate comparison.

density of all the samples at a longer time is much higher than Pt black. Comparing three samples having the highest current (5 h DEA, 7 h MEA and 9 h MEA), 5th hour DEA current density profile decays with respect to time, which later exhibited a steady current with respect to time. It is shown that small flower-like structures synthesised using DEA at the 5th hour tends to dissipate current, while bigger flower-like particles of 7th and 9th hour MEA able to limit current dissipation thereby maintaining the high current at a longer period.

4. Conclusion

Platinum hierarchical flower-like morphology was synthesised using amino alcohol as reducing agent. The amino derivatives (MEA and DEA) influence the Pt growth because they control the reducing rate in which particles synthesised with DEA induce a high reduction rate compared to MEA. The synthesis times play a vital role in the development of Pt anisotropic structures. It is worth to mention that both MEA and DEA exhibit significant results whereby the 7th hour is the optimum condition for MEA and 5th hour for DEA. Both produce different geometry and catalytic properties. A small flower-like structure is formed during 5th hour using DEA, which exhibited excellent catalytic activity, but experienced decaying of current at longer times. Contrariwise, the flower-like structures formed during the 7th hour using MEA, possess catalytic activity comparable to the commercial Pt black and exhibit greater stability at a longer period.

Acknowledgement

This work was supported by Universiti Sains Malaysia through Short Term Grant (304/PFIZIK/6313036). The author also would like

to thank Universiti Sains Malaysia and Ministry of Education Malaysia for financial scholarship as well as NanoBRI @ INFORMM for laboratory facilities.

References

[1] Y. Zhang, X. Bai, X. Wang, K.K. Shiu, Y. Zhu, H. Jiang, Highly sensitive Graphene–Pt nanocomposites amperometric biosensor and its application in living cell H_2O_2 detection, Anal. Chem. 86 (2014) 9459–9465.
[2] F.J. Nores-Pondal, I.M.J. Vilella, H. Troiani, M. Granada, S.R. de Miguel, O.A. Scelza, et al., Catalytic activity vs. size correlation in platinum catalysts of PEM fuel cells prepared on carbon black by different methods, Int. J. Hydrogen Energy 34 (2009) 8193–8203.
[3] A.L. Stepanov, A.N. Golubev, S.I. Nikitin, Y.N. Osin, A review on the fabrication and properties of platinum nanoparticles, Rev. Adv. Mater. Sci. 38 (2014) 160–175.
[4] B.S. Choi, S.M. Kim, J. Gong, Y.W. Lee, S.W. Kang, H.S. Lee, et al., One-pot self-templating synthesis of Pt hollow nanostructures and their catalytic properties for CO oxidation, Chem.A Eur. J. 20 (2014) 11669–11674.
[5] B.Y. Xia, H. Bin Wu, Y. Yan, X.W. (David) Lou, X. Wang, Ultrathin and ultralong single-crystal platinum nanowire assemblies with highly stable electrocatalytic activity, J. Am. Chem. Soc. 135 (2013) 9480–9485.
[6] Y. Li, Q. Wu, S. Jiao, C. Xu, L. Wang, Single Pt nanowire electrode: preparation, electrochemistry, and electrocatalysis, Anal. Chem. 85 (2013) 4135–4140.
[7] L. Wang, M. Imura, Y. Yamauchi, Tailored design of architecturally controlled Pt nanoparticles with huge surface areas toward superior unsupported Pt electrocatalysts, ACS Appl. Mater. Interfaces 4 (2012) 2865–2869.
[8] S. Mahima, R. Kannan, I. Komath, M. Aslam, V.K. Pillai, Synthesis of platinum Y-Junction nanostructures using hierarchically designed alumina templates and their enhanced electrocatalytic activity for fuel-cell applications, Chem. Mater. 20 (2007) 601–603.
[9] A. Dandapat, A. Mitra, P.K. Gautam, G. De, A facile synthesis of Pt nanoflowers composed of an ordered array of nanoparticles, Nanomater. Nanotechnol. 3 (2013) 1–7.
[10] X. Huang, Z. Zhao, J. Fan, Y. Tan, N. Zheng, Amine-assisted synthesis of concave polyhedral platinum nanocrystals having {411} High-Index facets, J. Am. Chem. Soc. 133 (2011) 4718–4721.
[11] Y. Xia, Y. Xiong, B. Lim, S.E. Skrabalak, Shape-controlled synthesis of metal nanocrystals: simple chemistry meets complex physics? Angew. Chem. Int. Ed. Engl. 48 (2009) 60–103.
[12] B.J. Hornstein, R.G. Finke, Transition-metal nanocluster kinetic and mechanistic studies emphasizing nanocluster agglomeration: demonstration of a kinetic method that allows monitoring of all three phases of nanocluster formation and aging, Chem. Mater 16 (2003) 139–150.
[13] S. Vedantam, V. Ranade, Crystallization: key thermodynamic, kinetic and hydrodynamic aspects, Sadhana 38 (2013) 1287–1337.
[14] M. Birkholz, Thin Film Analysis by X-Ray Scattering, WILEY-VCH Verlag GmbH & Co. KGaA, 2006.
[15] N.M. Dixit, C.F. Zukoski, Nucleation rates and induction times during colloidal crystallization: links between models and experiments, Phys. Rev. E 66 (2002) 051602, 1-051602-10.
[16] L. Ramajo, R. Parra, M. Reboredo, M. Castro, Preparation of amine coated silver nanoparticles using triethylenetetramine, J. Chem. Sci. 121 (2009) 83–87.
[17] F. Gloaguen, J.M. LéGer, C. Lamy, Electrocatalytic oxidation of methanol on platinum nanoparticles electrodeposited onto porous carbon substrates, J. Appl. Electrochem. 27 (1997) 1052–1060.
[18] P. Daubinger, J. Kieninger, T. Unmussig, G.A. Urban, Electrochemical characteristics of nanostructured platinum electrodes - a cyclic voltammetry study, Phys. Chem. Chem. Phys. 16 (2014) 8392–8399.
[19] J.N. Tiwari, F.M. Pan, K.L. Lin, Facile approach to the synthesis of 3D platinum nanoflowers and their electrochemical characteristics, New J. Chem. 33 (2009) 1482–1485.
[20] E. Broaddus, A. Wedell, S.A. Gold, Formic acid electrooxidation by a platinum nanotubule array electrode, Int. J. Electrochem. 2013 (2013) 1–7.
[21] S. Sun, G. Zhang, D. Geng, Y. Chen, R. Li, M. Cai, X. Sun, A Highly durable platinum nanocatalyst for proton exchange membrane fuel cells: multiarmed starlike nanowire single Crystal, Angew. Chem. Int. Ed. 50 (2011) 422–426.
[22] M.S. El-Deab, A.M. Mohammad, G.A. El-Nagar, B.E. El-Anadouli, Impurities contributing to catalysis: enhanced electro-oxidation of formic acid at Pt/GC electrodes in the presence of vinyl acetate, J. Phys. Chem. C 118 (2014) 22457–22464.
[23] I. Zaafarany, H. Boller, Electrochemical behavior of copper electrode in sodium hydroxide solutions, Curr. World Env. 4 (2009) 277–284.